

Evaluation Of Selected Radius Of Curvature Methods For Applications In Rounded Edge Diffraction Loss Computation

Chinyere Rosemary Ngwu¹

Department of Computer Engineering
Michael Okpara University of Agriculture,
Abia State

Kalu Constance²

Department of Electrical/Electronic and
Computer Engineering, University of Uyo,
Akwa Ibom, Nigeria

Kufre M. Udofia³

Department of Electrical/Electronic and
Computer Engineering, University of Uyo,
Akwa Ibom, Nigeria

Abstract—In this paper, evaluation of selected radius of curvature methods for applications in rounded edge diffraction loss computation is presented. Particularly, three methods are considered in the study and they are; one, exact radius method which is exact radius of curvature by manual curve fitting drawing approach, two, occultation distance method I which is radius of curvature by the occultation distance approximate expression and three, occultation distance method II. The analysis was conducted for the following values of occultation distance to path length ratios; 0.92, 0.5634, 0.491, 0.32 and 0. The results showed that the approximate radius of curvature by the occultation distance method I is very close to the exact radius of curvature (with error $\leq 0.05\%$) in all the cases of the occultation distance to path length ratios considered in the study. On the other hand, the occultation distance method II has error that increased up to 4.7 % when the occultation distance to path length ratio was 0.92. Also, the radius of curvature was undefined when the occultation distance to path length ratio is 0. In essence, the occultation distance method I can be used as a reliable approximate solution for finding the radius of curvature of rounded edge obstructions. Also, the results show that the radius of curvature is highest when the path length is half the occultation distance. In addition, the radius of curvature tends to zero (0) when occultation distance is zero or when occultation distance is equal to the path length.

Keywords— *Occultation Distance, Diffraction Loss, Radius Of Curvature, Path Length, Exact Radius Method, Rounded Edge Diffraction Loss*

1. INTRODUCTION

Wireless communication links are prone to diverse losses in the signal strength among which are the free space path loss, multipath fading, rain attenuation and also diffraction loss due to obstruction in the signal path [1,2,3,4,5,6,7,8,9,10]. Studies have shown that the amount of diffraction loss suffered by wireless signal depends on the shape and location of the obstruction relative to the path

length of the link [11,12,13,14,15,16]. In this case, the path length is the distance measure from the transmitter to the receiver.

Furthermore, researchers have identified single knife edge and rounded edge models as forms of approximations for different kinds of isolated obstructions for the computation of diffraction losses in wireless communication links [17,18,19,20,21,22,23,24]. Single knife edge model is applied when the obstruction has sharp or pointed edge at its apex point [25,26,27,28,29,30,31]. On the other hand, mountains and buildings can be modelled as rounded edge obstruction [32,33,34,35,36]. In this case, a rounded edge need to be fixed towards the vicinity of the apex of the obstruction and the radius of the rounded edge is used to estimate the additional diffraction loss due to the rounded edge obstruction.

In this paper, three different methods of calculating the radius of curvature of the rounded edge obstruction is presented. The three methods are also used to determine the radius of curvature for different shapes of the obstruction. The difference in the shape of the obstruction is defined in terms of the ratio of the occultation distance to the path length. The study seeks to establish the approximate solution approach that is more accurate for determination of the radius of curvature of rounded edge obstructions.

2.1 EXACT RADIUS OF CURVATURE BY MANUAL CURVE FITTING DRAWING APPROACH

Exact radius of curvature was obtained using the following geometry math set drawing tools which includes; ruler, 180° protractor, 45° set square, 60° set square and metal drawing compass. The math drawing tools were used to draw tangent lines from the two end points P_{e1} and P_{e2} of the elevation profile and the two tangent lines intersect near the elevation profile apex, denoted as point Pvt in Figure 1. Then, a perpendicular line was drawn at each of the two tangent points, P_{t1} and P_{t2} on the elevation profile and the intersection of the two perpendicular lines forms the centre (denoted as Pc) of the circle and the distance from the centre to any of the two tangent points gives the required radius of curvature, denoted here as R_{extM} , where R_{extM} is the length of line from point Pc to Pt1 or the line from point Pc to Pt2.

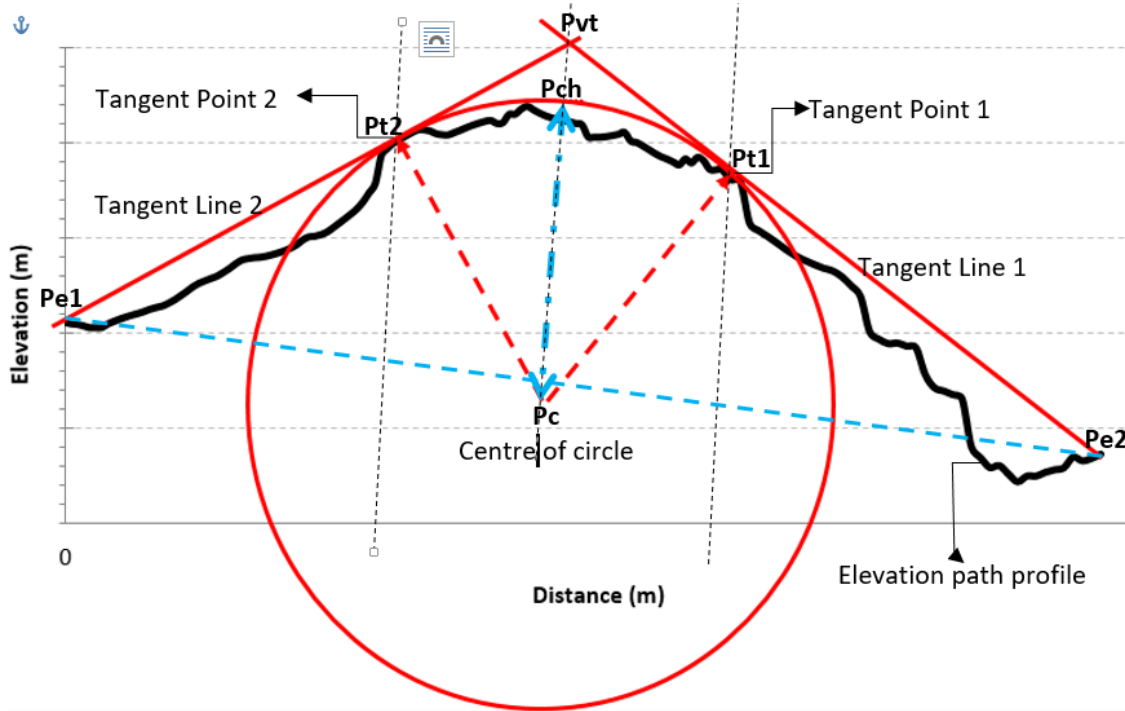


Figure 1. The geometry used for the calculation of radius of curvature of the rounded edge obstruction

2.2 RADIUS OF CURVATURE BY OCCULTATION DISTANCE APPROXIMATE EXPRESSION METHOD I

This method uses the occultation distance, D_{OCC} and a parameter, α to determine the radius of curvature, denoted as R_{OCCM} ;

$$R_{OCCM} = \frac{D_{OCC}}{\alpha} \quad (1)$$

Where

$$D_{OCC} = |P_{t2,hor} - P_{t1,hor}| \quad (3)$$

Where $P_{t2,hor}$ and $P_{t1,hor}$ the horizontal distance of the tangent points P_{t2} and P_{t1} from the origin.

$$\alpha = \cos^{-1} \left(\frac{(L_{TR}^2) + (L_{RV}^2) - (L_{TV}^2)}{2(L_{TR})(L_{RV})} \right) \quad (2)$$

L_{TR} is the path length of the line from endpoint P_{e1} to endpoint P_{e2}

L_{TV} is the length of the line from the vertex point, P_{vt} to endpoint P_{e1}
 L_{RV} is the length of the line from the vertex point, P_{vt} to endpoint P_{e2}

2.3 RADIUS OF CURVATURE BY THE OCCULTATION DISTANCE APPROXIMATE EXPRESSION METHOD II

The second method for computing the radius of curvature based on the occultation distance is given as;

$$R = \frac{2(D_{OCC})(d1)(d2)}{(\alpha)[(d1^2) + (d2^2)]} \quad (3)$$

The elevation profile of Figure 3 is used for the case study hilly terrain .

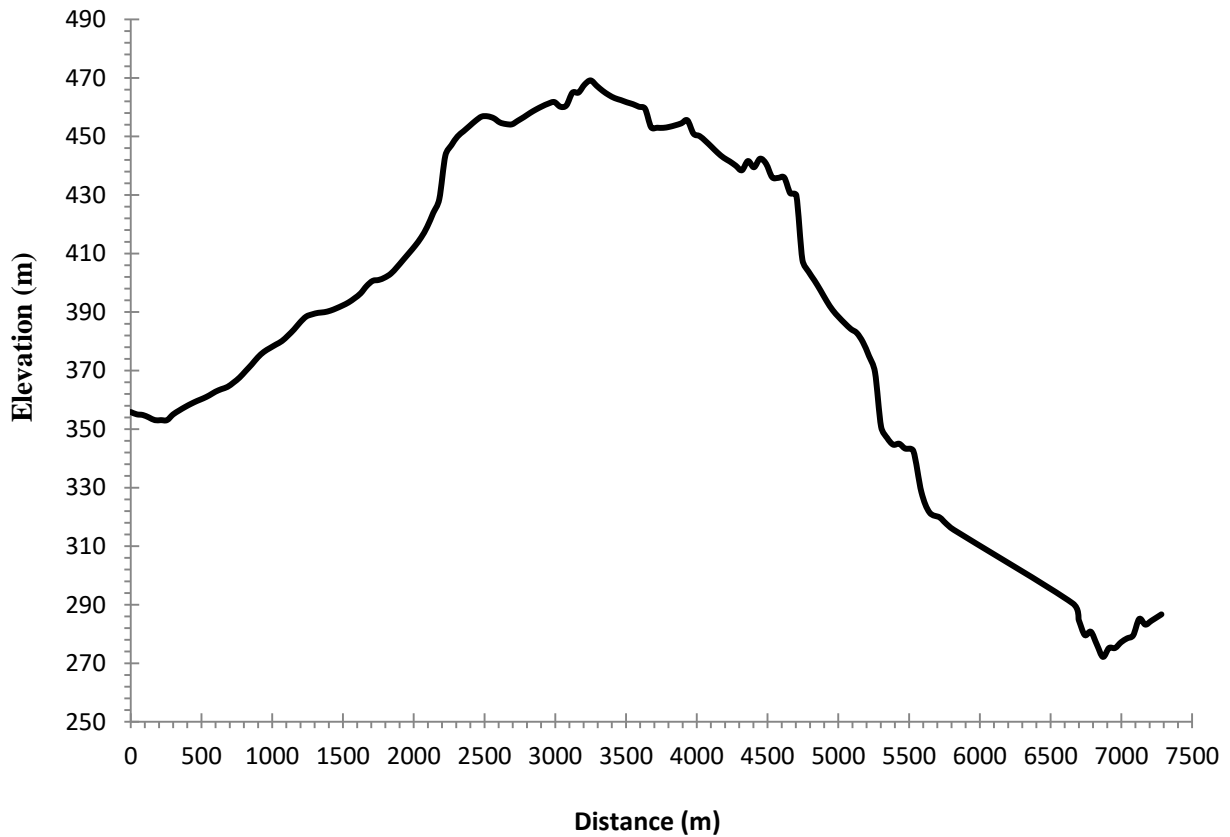


Figure 2 The Elevation Profile Data For The Case Study Hilly Terrain

3. Results and discussion

Based on the given elevation profile data, the path length in meters, $d(m)$ is 7,283.41 m, the occultation distance, $D(m)$ is 2,310.76, the angle α is 0.050304655 radians and the signal frequency is 1GHz. The radius of curvature computed using the three different methods for the case where the occultation distance to path length ratio, $\frac{D(m)}{d(m)}$ is 0.32 are presented in Table 1 and Figure 3. The results in Figure 3 and Table 1 show that at $\frac{D(m)}{d(m)} = 0.32$ the radius of curvature computed by the occultation distance method II is the lowest with a value of 23561.2 m which is 0.9 %

lower than the radius of curvature value of 23783.7 m obtained by the exact radius method. The radius of curvature computed using the three different methods for the case where the occultation distance to path length ratio, $\frac{D(m)}{d(m)}$ is 0.92 are given in Table 2 and Figure 4. The results in Figure 4 and Table 2 show that at $\frac{D(m)}{d(m)} = 0.92$ the radius of curvature computed by the occultation distance method I I is the lowest with a value of 8,333.09 m which is 4.7 % lower than the radius of curvature value of 8,740.98 m obtained by exact radius method.

Table 1 The radius of curvature computed using the three different methods for the case where the occultation distance to path length ratio, $\frac{D(m)}{d(m)}$ is 0.32

Methods For Computation of the Rounded Edge Radius	R (m)	Normalized radius of curvature with respect to that computed with the exact radius method (%)
Exact radius Method	23783.7	100.0
Occultation Distance Method I	23769.2	99.9
Occultation Distance Method I I	23561.2	99.1

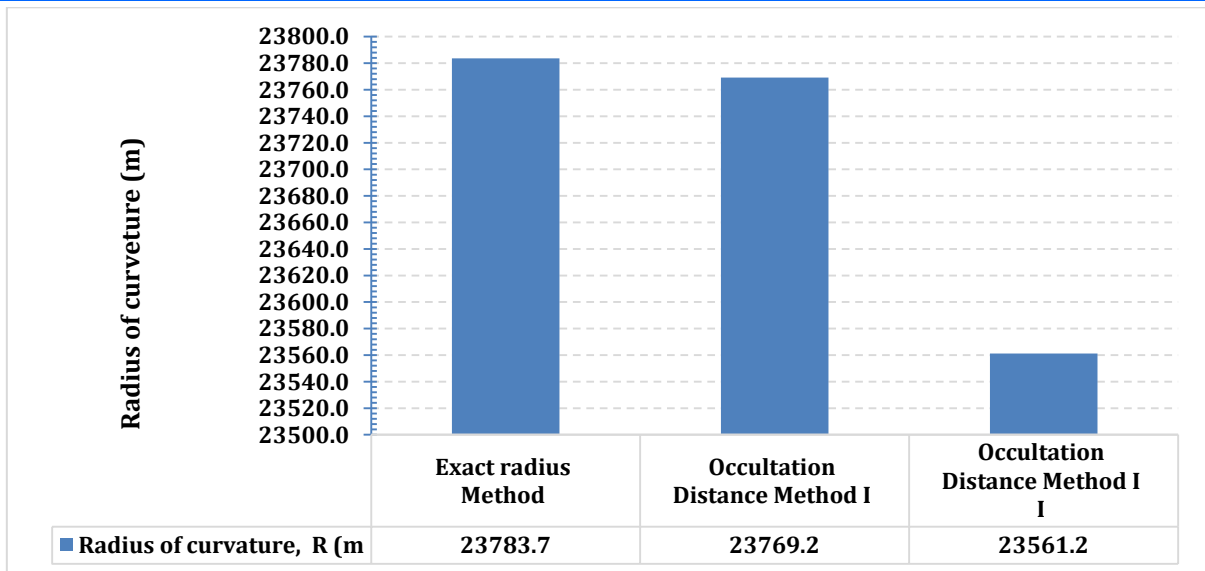


Figure 3 The bar chart the radius of curvature computed using the three different methods for the case where the occultation distance to path length ratio, $\frac{D(m)}{d(m)}$ is 0.32

Table 2 The radius of curvature computed using the three different methods for the case where the occultation distance to path length ratio, $\frac{D(m)}{d(m)}$ is 0.92

Methods For Computation of the Rounded Edge Radius	Radius of curvature, R (m)	Normalized radius of curvature with respect to that computed with the exact radius method (%)
Exact radius Method	8,740.98	100.00
Occultation Distance Method I	8,723.18	99.80
Occultation Distance Method I I	8,333.09	95.33

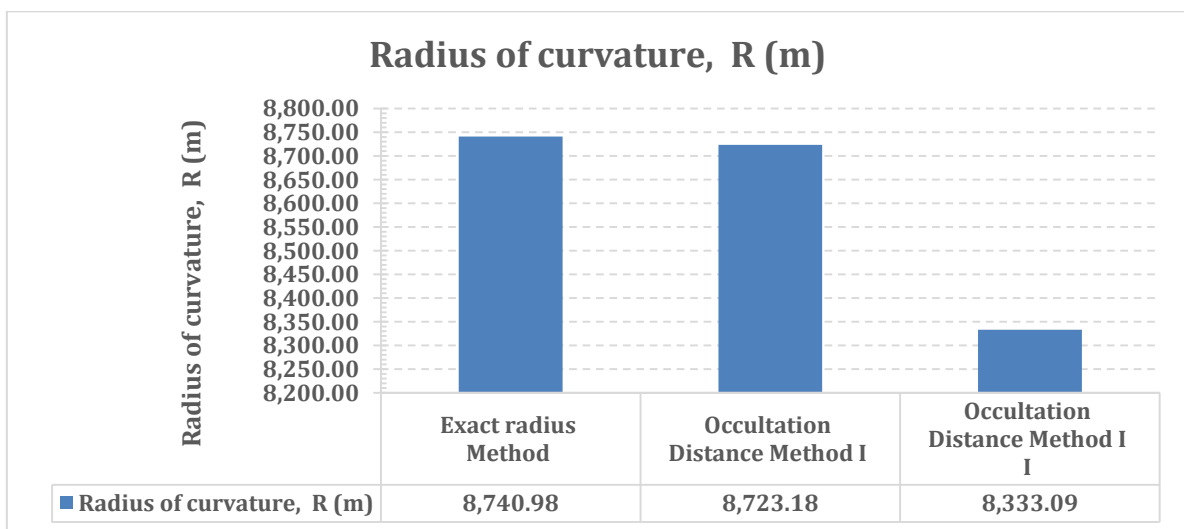


Figure 4 The bar chart the radius of curvature computed using the three different methods for the case where the occultation distance to path length ratio, $\frac{D(m)}{d(m)}$ is 0.92

The radius of curvature computed using the three different methods for the case where the occultation distance to path length ratio, $\frac{D(m)}{d(m)}$ is 0.5634 are given in Table 3 and Figure

26690.86 m which is 1.3 % lower than the radius of curvature value of 27039.35 m obtained by exact radius method.

5. The results in Figure 5 and Table 3 show that at $\frac{D(m)}{d(m)} = 0.5634$ the radius of curvature computed by the occultation distance method II is the lowest with a value of

Table 3 The radius of curvature computed using the three different methods for the case where the occultation distance to path length ratio, $\frac{D(m)}{d(m)}$ is 0.5634

Methods For Computation of the Rounded Edge Radius	Radius of curvature, R (m)	Normalized radius of curvature with respect to that computed with the exact radius method (%)
Exact radius Method	27039.35	100.00
Occultation Distance Method I	27025.54	99.95
Occultation Distance Method I I	26690.86	98.71

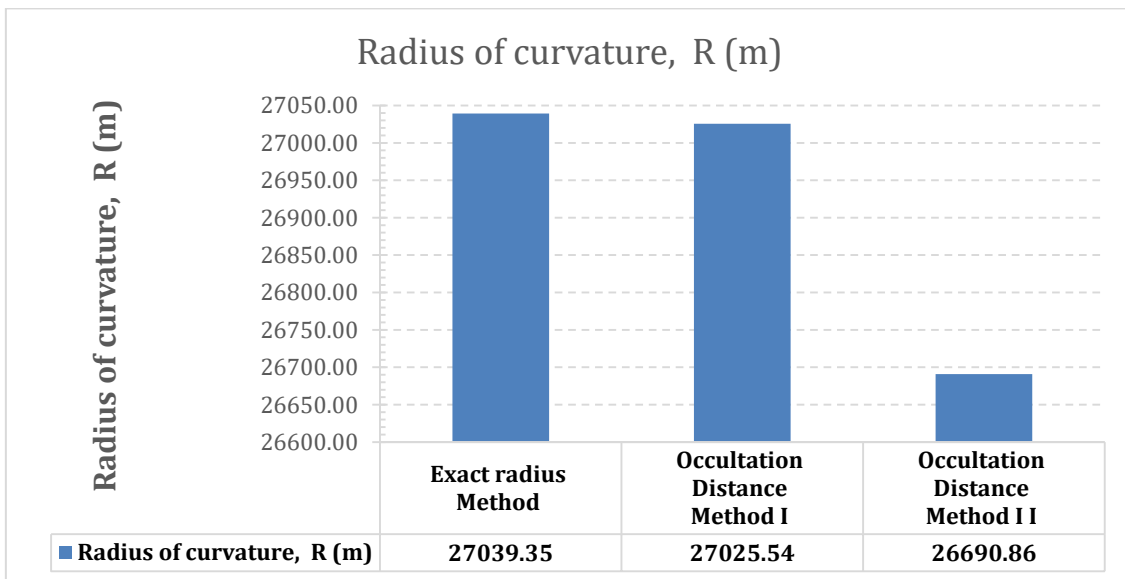


Figure 5 The bar chart the radius of curvature computed using the three different methods for the case where the occultation distance to path length ratio, $\frac{D(m)}{d(m)}$ is 0.5634

The radius of curvature computed using the three different methods for the case where the occultation distance to path length ratio, $\frac{D(m)}{d(m)}$ is 0.4910 are given in Table 4 and Figure

occultation distance method I I is the lowest with a value of 27298.95 m which is 0.6 % lower than the radius of curvature value of 27457.14 m obtained by exact radius method.

6. The results in Figure 6 and Table 4 show that at $\frac{D(m)}{d(m)} = 0.4910$ the radius of curvature computed by the

Table 4 The radius of curvature computed using the three different methods for the case where the occultation distance to path length ratio, $\frac{D(m)}{d(m)}$ is 0.4910

Methods For Computation of the Rounded Edge Radius	Radius of curvature, R (m)	Normalized radius of curvature with respect to that computed with the exact radius method (%)
Exact radius Method	27457.14	100.00
Occultation Distance Method I	27443.09	99.95
Occultation Distance Method I I	27298.95	99.42

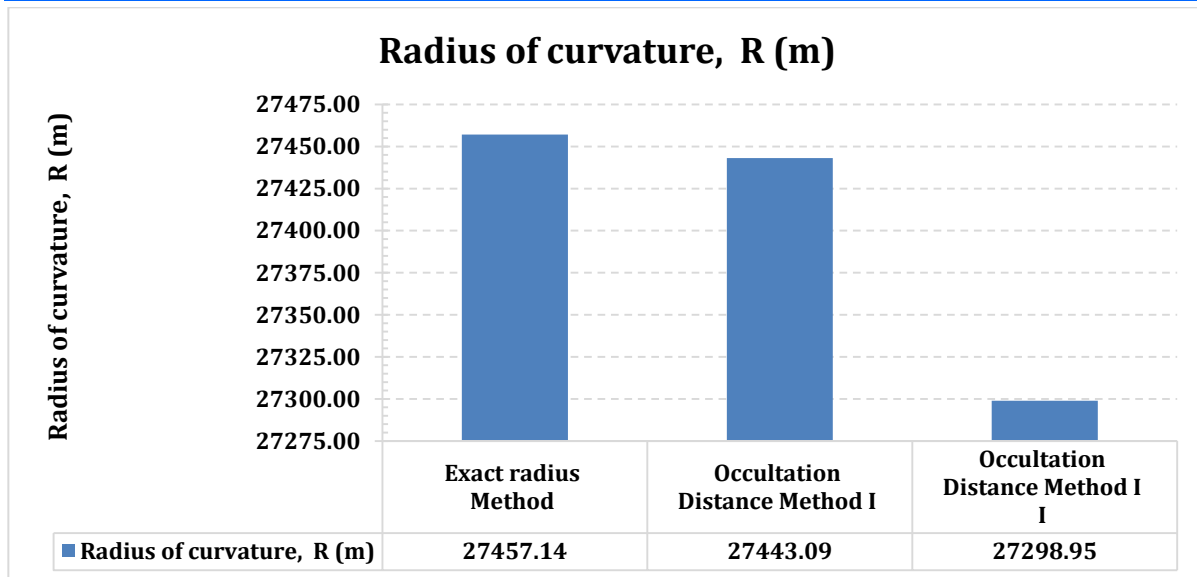


Figure 6 The bar chart the radius of curvature computed using the three different methods for the case where the occultation distance to path length ratio, $\frac{D(m)}{d(m)}$ is 0.4910

The radius of curvature computed using the three different methods for the case where the occultation distance to path length ratio, $\frac{D(m)}{d(m)}$ is 0 are given in Table 5. The results in Figure Table 5 show that at $\frac{D(m)}{d(m)} = 0$ the radius of curvature computed by the occultation distance method I I is undefined while the radius of curvature obtained by exact radius method and the occultation distance method I are both 0.

In all, the approximate radius of curvature by the occultation distance Method I is very close (error $\leq 0.05\%$) to the exact radius of curvature in all the cases of the occultation distance to path length ratios considered in the study. On the other hand, the occultation distance method II

has error that increased up to 4.7 % when $\frac{D(m)}{d(m)}$ is 0.92.

Also, the radius of curvature was undefined when $\frac{D(m)}{d(m)}$ is 0. In essence, the occultation distance method I can be used as a reliable approximate solution for finding the radius of curvature of rounded edge obstructions.

Furthermore, the graph plot of the radius of curvature by exact radius method versus occultation distance to path length ratio, $\frac{D(m)}{d(m)}$ for the exact radius method is given in Figure 7. The results in Figure 7 show that the radius of curvature is highest when the path length is half the occultation distance. The radius of curvature tends to zero (0) when occultation distance is zero or when occultation distance is equal to the path length.

Table 5 The radius of curvature computed using the three different methods for the case where the occultation distance to path length ratio, $\frac{D(m)}{d(m)}$ is 0

Methods For Computation of the Rounded Edge Radius	Radius of curvature, R (m)
Exact radius Method	0
Occultation Distance Method I	0
Occultation Distance Method I I	Undefined

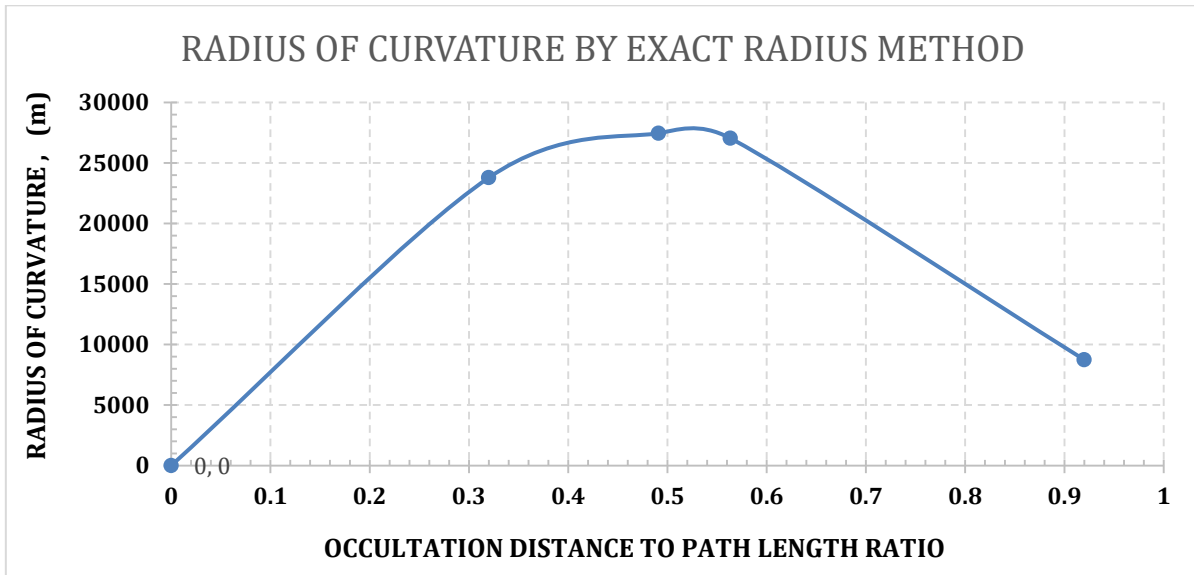


Figure 7 Radius of curvature by exact radius method versus occultation distance to path length ratio, $\frac{D(m)}{d(m)}$ for the exact radius method

4. Conclusion

Three different methods of computing radius of curvature for rounded edge diffraction loss calculation are presented. The three methods are examined under different cases of occultation distance to path length ratios. The results show that the occultation distance method I is a reliable approximate solution for finding the radius of curvature of rounded edge obstructions. Also, the results show that the radius of curvature is highest when the path length is half the occultation distance. In addition, the radius of curvature tends to zero (0) when occultation distance is zero or when occultation distance is equal to the path length.

References

- Maxama, X. B., & Markus, E. D. (2018, October). A Survey on Propagation Challenges in Wireless Communication Networks over Irregular Terrains. In *2018 Open Innovations Conference (OI)* (pp. 79-86). IEEE.
- Budalal, A. A., Rafiqul, I. M., Habaebi, M. H., & Rahman, T. A. (2019). The effects of rain fade on millimetre wave channel in tropical climate. *Bulletin of Electrical Engineering and Informatics*, 8(2), 653-664.
- Wei, L., Hu, R. Q., Qian, Y., & Wu, G. (2014). Key elements to enable millimeter wave communications for 5G wireless systems. *IEEE Wireless Communications*, 21(6), 136-143.
- Han, C., Wu, Y., Chen, Z., & Wang, X. (2019). Terahertz communications (TeraCom): Challenges and impact on 6G wireless systems. *arXiv preprint arXiv:1912.06040*.
- Shamsan, Z. A. (2020). Rainfall and Diffraction Modeling for Millimeter-Wave Wireless Fixed Systems. *IEEE Access*, 8, 212961-212978.
- Morais, D. H. (2020). The Mobile Wireless Path. In *Key 5G Physical Layer Technologies* (pp. 41-74). Springer, Cham.
- Uzairue, S. I. (2016). Determination and Analysis of Signal/Path-Loss Exponent.
- Picallo, I., Klaina, H., Lopez-Iturri, P., Aguirre, E., Celaya-Echarri, M., Azpilicueta, L., ... & Alejos, A. (2019). A radio channel model for D2D communications blocked by single trees in forest environments. *Sensors*, 19(21), 4606.
- Femi-Jemilohun, O. J., & Walker, S. (2014). Performance Evaluation of 24GHz Spectrum Indoor Wireless Radio Links. *International Journal of Emerging Technology and Advanced Engineering*, 4(11).
- Rappaport, T. S., Xing, Y., Kanhere, O., Ju, S., Madanayake, A., Mandal, S., ... & Trichopoulos, G. C. (2019). Wireless communications and applications above 100 GHz: Opportunities and challenges for 6G and beyond. *Ieee Access*, 7, 78729-78757.
- Eduediuyai, D., Enyenihi, J., & Markson, I. (2019). Analysis of the Effect of Variations in Refractivity Gradient on Line of Sight Percentage Clearance and Single Knife Edge Diffraction Loss. *International Journal of Sustainable Energy and Environmental Research*, 8(1), 1-9.
- Bai, T., Vaze, R., & Heath, R. W. (2014). Analysis of blockage effects on urban cellular networks. *IEEE Transactions on Wireless Communications*, 13(9), 5070-5083.
- Bai, T., & Heath, R. W. (2014). Coverage and rate analysis for millimeter-wave cellular networks. *IEEE Transactions on Wireless Communications*, 14(2), 1100-1114.
- Zhang, J., Ge, X., Li, Q., Guizani, M., & Zhang, Y. (2016). 5G millimeter-wave antenna array: Design and challenges. *IEEE Wireless communications*, 24(2), 106-112.
- Rappaport, T. S., Xing, Y., Kanhere, O., Ju, S., Madanayake, A., Mandal, S., ... & Trichopoulos, G. C. (2019). Wireless communications and applications above 100 GHz: Opportunities and challenges for 6G and beyond. *Ieee Access*, 7, 78729-78757.
- Picallo, I., Klaina, H., Lopez-Iturri, P., Aguirre, E., Celaya-Echarri, M., Azpilicueta, L., ... & Alejos, A. (2019). A radio channel model for

- D2D communications blocked by single trees in forest environments. *Sensors*, 19(21), 4606.
17. Oluropo, O. E., Ezeh, I. H., & Nkwocha, C. P. (2017). Determination of Diffraction Loss over Isolated Doubled Edged Hill Using the ITU-R P. 526-13 Method for Rounded Edge Diffraction. *American Journal of Software Engineering and Applications*, 6(2), 56-60.
 18. Chikezie, A., Uko, M. C., & Nwokonko, S. C. (2017). Comparative Analysis of the Impact of Frequency on the Radius of Curvature of Single and Double Rounded Edge Hill Obstruction. *Mathematical and Software Engineering*, 3(2), 164-172.
 19. Kasampalis, S. (2018). *Modelling and coverage improvement of DVB-T networks* (Doctoral dissertation, Brunel University London).
 20. Ghasemi, A., Abedi, A., & Ghasemi, F. (2016). Terrestrial Mobile Radio Propagation. In *Propagation Engineering in Wireless Communications* (pp. 217-289). Springer, Cham.
 21. Brummer, A., Deinlein, T., Hielscher, K. S., German, R., & Djanatliev, A. (2018, December). Measurement-Based Evaluation of Environmental Diffraction Modeling for 3D Vehicle-to-X Simulation. In *2018 IEEE Vehicular Networking Conference (VNC)* (pp. 1-8). IEEE.
 22. Savazzi, S., Sigg, S., Nicoli, M., Rampa, V., Kianoush, S., & Spagnolini, U. (2016). Device-free radio vision for assisted living: Leveraging wireless channel quality information for human sensing. *IEEE Signal Processing Magazine*, 33(2), 45-58.
 23. Hamza, M. G., Latiff, L. A., Mustafa, E. M., & Gasim, W. M. (2017, January). Radio propagation and troposphere parameters effect for Microwave links in Sudan. In *2017 International Conference on Communication, Control, Computing and Electronics Engineering (ICCCCEE)* (pp. 1-5). IEEE.
 24. Ghasemi, A., Abedi, A., & Ghasemi, F. (2016). Line-of-Sight Propagation. In *Propagation Engineering in Wireless Communications* (pp. 291-359). Springer, Cham.
 25. Jude, O. O., Jimoh, A. J., & Eunice, A. B. (2016). Software for Fresnel-Kirchoff single knife-edge diffraction loss model. *Mathematical and Software Engineering*, 2(2), 76-84.
 26. Ezenugu, I. A., Edokpolor, H. O., & Chikwado, U. (2017). Determination of single knife edge equivalent parameters for double knife edge diffraction loss by Deygout method. *Mathematical and Software Engineering*, 3(2), 201-208.
 27. Samuel, W., Nwaduwa, F. O. C., & Oguichen, T. C. (2017). Algorithm for Computing N Knife Edge Diffraction Loss Using Epstein-Peterson Method. *American Journal of Software Engineering and Applications*, 6(2), 40-43.
 28. Brown, T. W., & Khalily, M. (2018). Integrated shield edge diffraction model for narrow obstructing objects. *IEEE Transactions on Antennas and Propagation*, 66(12), 6588-6595.
 29. Ezeh, I. H., & Nwokonko, S. C. (2017). Determination of Single Knife Edge Equivalent Parameters for Triple Knife Edge Diffraction Loss by Giovanelli Method. *International Journal of Information and Communication Sciences*, 2(1), 10.
 30. Imoh-Etefia, U. E., Simeon, O., & Utibe-Abasi, S. B. Analysis Of Obstruction Shadowing In Bullington Double Knife Edge Diffraction Loss Computation.
 31. Nnadi, N. C., Jacob, H. A., & Eze, G. N. (2020). LINK BUDGET ANALYSIS FOR LINE OF SIGHT WIRELESS COMMUNICATION LINK WITH KNIFE EDGE DIFFRACTION OBSTRUCTION. In *practice*, 4(6).
 32. Amadi, C. H., Kalu, C., & Udofia, K. (2020). Modelling of Bit Error Rate as a Function of Knife Edge Diffraction Loss Based on Line of Sight Percentage Clearance. *International Journal of Engineering & Technology*, 5(1), 9-24.
 33. Ozuomba, S., Kalu, C., & Enyenih, H. J. Comparative Analysis of the Circle Fitting Empirical Method and the International Telecommunication Union Parabola Fitting Method for Determination of the Radius of Curvature for Rounded Edge Diffraction Obstruction. *Communications*, 7, 16-21.
 34. Uko, M. C., Udoka, U. E., & Nkwocha, C. P. (2017). Parametric Analysis of Isolated Doubled Edged Hill Diffraction Loss Based on Rounded Edge Diffraction Loss Method and Different Radius of Curvature Methods. *Mathematical and Software Engineering*, 3(2), 217-225.
 35. Simeon, O., SF, E. O., & Olumide, B. M. (2018). Development of Mathematical Models and Algorithms for Exact Radius of Curvature Used in Rounded Edge Diffraction Loss Computation. *Development*, 5(12).
 36. Ezenugu, I. A., Edokpolor, H. O., & Chikwado, U. (2017). Determination of single knife edge equivalent parameters for double knife edge diffraction loss by Deygout method. *Mathematical and Software Engineering*, 3(2), 201-208.